Characterization of Piezoelectric Bimorph Actuator 3D-Deformations Caused by Electric Change by Means of Multiscale Curvature Analysis

Tomasz BARTKOWIAK, Marcin PELIC
Poznan University of Technology, ul. Piotrowo 3, 60-965 Poznań,
tomasz.bartkowiak@put.poznan.pl, marcin.pelic@put.poznan.pl

Abstract

The objective of this work is to demonstrate the use of multiscale curvature tensor analysis to characterize deformations of piezoelectric bimorph actuator and to study the relation between loaded electric charge and the resulting deformed surface curvature. In particular, the strength of the correlations between surface shape characterized by curvature parameters (i.e., principal, Gaussian or mean curvature) and charge density is sought. The impact that the scale of the analysis of the curvature can have on the values of the curvature parameters for the deformed surfaces and the correlation with discharge energy is also studied. In this study the deformations of piezoelectric bimorph actuators are studied. In order to achieve quasi-static measurements, a dedicated charge amplifier was built to supply charge to the actuator. The deformations were then measured by Polytec® 3D laser scanning vibrometer PSV-400 by integration of captured motion. The obtained data was used to calculate curvature tensor field at multiple scales by applying the normal-based method. Principal, mean and Gaussian curvature was calculated at multiple scales and were correlated with applied charge. The obtained results contribute to better understanding of piezoelectric behavior under electric field.

Keywords: piezoelectricity, curvature, multiscale analysis, laser scanning vibrometer

1. Introduction

The objective of this work is to demonstrate the use of multiscale curvature tensor analysis to characterize deformations of piezoelectric bimorph actuator and to study the relation between loaded electric charge and the resulting deformed surface curvature. In particular, the strength of the correlations between surface shape characterized by curvature parameters (i.e., principal, Gaussian or mean curvature) and charge density is sought. The impact that the scale of the analysis of the curvature can have on the values of the curvature parameters for the deformed surfaces and the correlation with is also studied.

The relation between surface curvature and charge accumulation is a well-studied phenomenon. Charge tends to accumulate at high curvature regions of a conductor [1]. Size-dependent coupling of charge-density with curvature is a phenomenon that is also studied in piezoelectricity. Hadjesfandiari et al. [2] presented a theory that describes coupling between the skew-symmetric mean curvature tensor and the polarization field, which allows for piezoelectric behavior.

Curvature is an important factor in ion-exchange membranes. Silver-plated Selemion shows controllable bending behavior under applied voltage for certain circumstances. In that case, the correlation between the charge and curvature could change when the environmental humidity changed. Recent studies present that this behavior is independent of humidity [3], placing more emphasis on the curvature. A similar phenomenon has been

noticed in charged membranes [4, 5]. In thin layers of semiconductors, i.e., superfluids, surface defects are repelled (attracted) by regions of positive (negative) Gaussian curvature. For liquid crystals, charges 0 and 4π are attracted by regions of positive curvature while all other charges are repelled [6]. In the manufacturing processes, surface curvatures are determined by discharge energy in EDM [7].

Most of the authors focus on theoretical modelling of deformation-charge density coupling. There is still very little research on experimental study of this phenomenon and characterization the effects at various scales.

Geometric properties of complex surfaces can change with the scale of observation, i.e., measurement or calculation [8]. Curvature, like area or length, naturally varies with scale. Because curvature is approximately the spatial derivative of the slope, it requires no datum, whereas heights or slopes do require a datum. This can be valuable when the datum is not obvious, such as in characterizing tomographic or vibrometer measurements. In addition, curvature can indicate convex and concave regions. The former are important in contact mechanics, and the latter can be significant in fatigue and in fracture mechanics. Curvature analysis can identify microgrooves and holes, which act as stress concentrators. It can be also helpful in identifying lay, or surface directionality, i.e., anisotropy, by analyzing the orientation of maximal and minimal curvature vectors. Finally, because curvature is a tensor, it is possible to calculate gradient, divergence, and curl, which can help in improved characterization of particular surfaces. The aforementioned features make curvature a prospective candidate for characterization of surface topographies. Some initial studies showed its good performance in the establishment of functional correlations between curvature of the highest asperities and coefficient of friction [9], in the characterization of topographic curvature in relation to discharge energy in microEDM process [10].

Apart from analysis of how geometric parameters like curvature, slope , length [11] or area [12] change with scale, there exist other approaches which allow multiscale characterizations. This include measurement of the same region with different instruments and optics, fractals, structure function [13], wavelets [14] and, morphological [15], Fourier transformation-based, and sliding bandpass filtration [8]. The first approach might be problematic due to differences in the measurement transfer functions between instruments, method-specific surface artifacts and dataset alignment issues. However, it is possible to investigate the surface using complementary or partially overlapping scales. For example, a surface might be captured at 10×, 20×, and 50× magnifications. Many features could be present across two or more of these measurements, although they might appear differently at different magnifications. When analyzing a single measured datasets, multiscale effect could be achieved by either down-sampling or applying filtration in order to extract features of particular size. The latter can be achieved by frequency-based filtration using e.g. bandpass Gaussian filter [16] or wavelets [17]. Historically, surface or profiles were considered fractal, which means that their geometric complexity might be characterized by a single number called fractal dimension [18]. Many examples of surface topographies, including manufactured and non-engineering surfaces, are frequently multifractal with respect to scale. Characterizing such surfaces with a single FD can result in missing important insights and understandings [19].

In this study, we concentrate of the geometrical analysis of the piezoelectric beam. Its deformations are caused by charge supplied via dedicated power source. They are measured with laser scanning vibrometer due to the oscillating character of the motion. The measurement data is extracted and characterized using multiscale curvature analysis. The correlation between particular curvature parameter and electric charge are tested using linear regression.

2. Materials and methods

In all the experiments, a standard commercial bimorph piezoelectric actuator (SMBA4510T05M from STEMINC Inc.) was used. The material and geometric properties are summarized in Table 1. Please note that PZT stands for lead zirconate titanate which is piezoelectric material. The beam was mounted in the cantilever configuration in a dedicated grip. Fixed end of the actuator was clamped between flat and v-shaped elements what allowed rotation at this point. Similar approach was presented in the study by Pelic et al. [20].

Table 1. Material properties of piezoelectric actuator

Property	Value
Elastic modulus PZT	72 GPa
Elastic modulus substrate	11 GPa
Density piezoelectric	7900 kg/m^3
Density substrate	8900 kg/m^3
Piezoelectric constant	270e-12 m/V
Electrical permittivity	3500 ε_0 (F/m)
Beam length/width	40/10 mm
Thicknesses PZT/substrate	0.1 mm/0.2 mm

To supply electric charge to piezo actuator, an amplifier was designed and built, based on APEX Microtechnology PA91, a dedicated integrated circuit. This is a MOSFET type operational power amplifier designed, especially, for piezoelectric drives. It is characterized by its high voltage rise rate of 300 V/μs and a maximum output voltage of 400 V and 200 mA current. The schematic view of the charge amplifier is presetented in Figure 1.

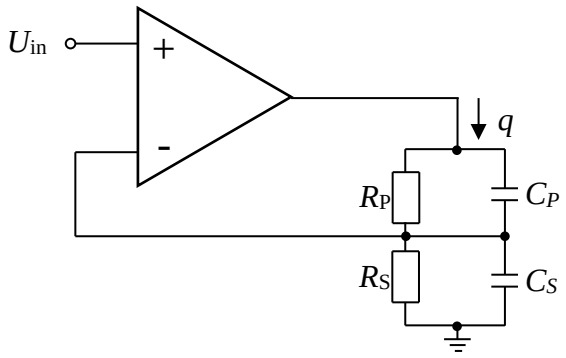

Figure 1. Electric scheme of the charge amplifier

The charge amplifier is an integrating element with high input impedance. C_p element in the diagram represents the substitute capacity of the piezo element. C_S capacity serves as a reference for measuring the charge accumulated in a piezo element.

In the ideal conditions (without R_P and R_S resistors) charge q can be denoted as:

$$q = U_{in} \cdot C_s. \tag{1}$$

For those conditions, the total gain of the amplifier can be expressed as:

$$k = \frac{C_s}{C_P}. \tag{2}$$

The main problem of charge amplifiers is their low output impedance and effect of dielectric drain current. It can be solved by connecting R_1 and R_2 resistors in the circuit. In order for these resistances not to cause drift in the low frequency range, the ratio of their resistance should be equal to the ratio of the capacitances of piezo element and measuring capacitor C_S,

$$\frac{R_S}{R_P} = \frac{C_s}{C_P}. \tag{3}$$

The parallel connection of those resistors converts the charge amplifier to a voltage amplifier operating below the frequency f_C:

$$f_c = \frac{1}{2\pi R_P C_P}. \tag{4}$$

In the actual system, the values of the passive electric components were selected so that the frequency f_C was 0.1 Hz, and the maximum current flowing in the circuit did not exceed the maximum current of the operational amplifier. A PCB (printed circuit board) was designed for the charge amplifier system (Figure 2 a) and its power supply. The assembled unit is shown in Figure 2 b.

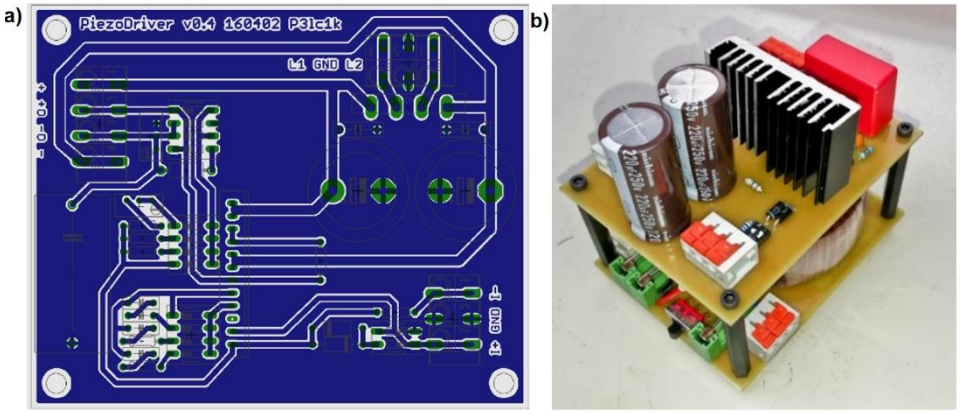

Figure 2. a) Overview of PCB, b) assembled charge amplifier.

The 3D deformations were measured by Polytec® 3D laser scanning vibrometer PSV-400 by integration of captured motion (Figure 3). The vibrometer offers non-contact testing of vibrations of individual points, paths or surfaces in three orthogonal axes. The measurement is performed on the basis of probing the instantaneous speed of individual points. The difference in the wavelength emitted from the laser source and the reflected wave from the tested surface is related to the instantaneous speed of the tested point, which is described by the Doppler effect. The tested element is not burdened with the mass of sensors and cabling, which is particularly important for testing vibrations generated by low mass objects, e.g. piezoelectric beam drives. Due to the nature of the Doppler phenomenon and the design of the vibrometer only a single point on the surface of piezoelement is measured at the a single moment. Maximum acquisition rate is 30 points per second. For the purpose of the test, one scanning head was used, which meant measuring the vibration speed of designated points in the axis parallel to the laser beam. In postprocessing, the vibration velocity of individual points is synchronized with others, creating a coherent image of vibrating virtual surfaces. In the presented case, the reference value used by the vibrometer, was the signal from the generator supplied to the piezoelectric element to put it in motion.

Two types of tests were performed. Firstly, piezo element was supplied with white noise. This allowed to determine normal modes of vibrations and their natural frequencies. Renderings of resulted 3D deformations of piezoelectric actuator, were presented in Figure 4 a). The data was then decomposed using Fourier transform to obtain first three modes of vibrations (fig. 4 b-d). First and third mode represent torsional vibrations of low amplitude, whereas second mode is bending direction with its natural frequency of 42 Hz. At this frequency, maximum deflection of the actuator was twice the permittable level according to the technical specifications of the beam.

The second types of tests were performed at supplying the piezoelement with sinusoidal voltage at 45 Hz. In this frequency, the bending character of oscillations was evident without risking of element destruction. Five different voltages, between 11 and 19 V, were applied (Table 2). Charge q can be calculated for each scenario by applying

formula (1). The measurement area used for further analysis was 1090×260 μm (218×104 points). Sampling intervals in x and y were 5 and 2.5 μm respectively. Only the maximum positions of the beams during oscillation was considered for each case.

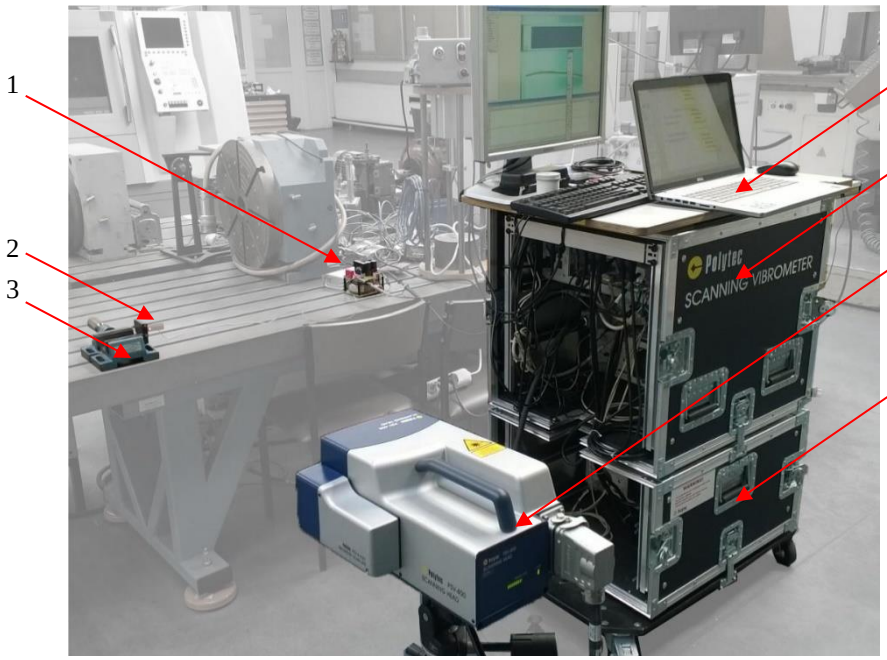

Figure 3. Test stand with vibrometer: 1) charge amplifier, 2) piezoelectric actuator, 3) grip, 4) laptop, 5) vibrometer control unit and PC, 6) scanning head, 7) measurement amplifiers

In this paper, the shape of deformed piezoelectric actuator is characterized by its curvatures. Intuitively, the curvature is the amount by which surface deviates from being a plane. In other words, the curvature is a measure of the instantaneous rate of change of direction of a point that moves on the curve: the larger the curvature, the larger this rate of change [21]. Curvature approach is more detailed than comparing just the amplitude of deformations or their derivatives as it allows calculation of curvature at a specific location on the actuator under charge. This can be done at various scales which can be attributed with size of particular surface features. Fine scale characterizations refer to the geometric features of smallest dimensions (which can be attributed to noise, roughness or waviness), whereas large scale are attributed to general form (or shape) of the measured surface. The concept of multiscale analysis, including geometric like curvature was presented by Brown et al. [8].

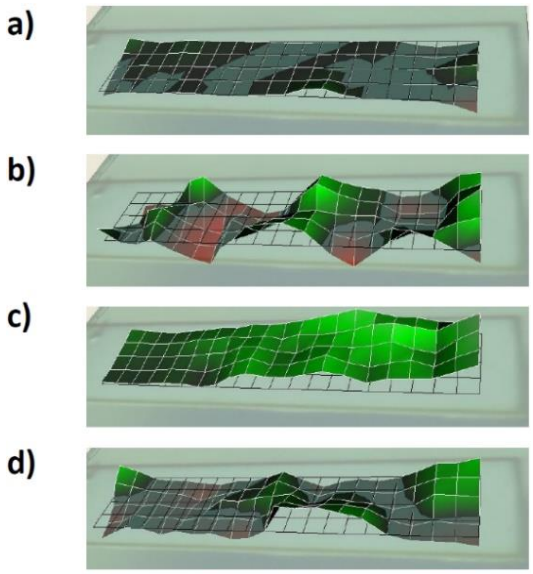

Figure 4. 3D deformations caused by white noise: a) the entire bandwidth (0−4 kHz) b) 13 Hz, c) 42 Hz and d) 300 Hz

In this study, curvatures are calculated using a 3D normal-based method. The measurement data are represented as a function $z=f(x,y)$. First at each scale and at each location three surface normals have to be computed from measured heights in the neighborhood surrounding that location. Then the curvatures are calculated from the normal. The scale is adjusted by changing the size of the region over which the normals are calculated. Changing the size of the region influences the current sampling interval for normal estimation and tiling. However, fixed number of points for normal estimation, equal to nine, remains.

The covariance matrix method is used for computing the normals. For each location and at each scale the closest 3×3 neighborhood of heights is used for computing the normal vectors. The heights at the edges are excluded from further analysis because these could be prone to error, as limited number of points, less than nine, can only be used for computations. Detailed description of the curvature estimation technique used in this study is given in [10, 22].

Table 2. Set up parameters for five test scenarios

Number of scenario	Frequency [Hz]	Voltage [V]	Charge [μC]
1	45	11	74.8
2	45	13	88.4
3	45	15	102.0
4	45	17	115.6
5	45	19	129.2

The curvature tensor **T** is a symmetric 3×3 matrix that can be expressed as a product:

$$\mathbf{T} = \mathbf{P} \cdot \mathbf{D} \cdot \mathbf{P}^{-1} \tag{5}$$

where: $\mathbf{P} = (\mathbf{k_1}, \mathbf{k_2}, \mathbf{n})$ and

$$\mathbf{D} = \begin{pmatrix} \kappa_1 & 0 & 0 \\ 0 & \kappa_2 & 0 \\ 0 & 0 & 0 \end{pmatrix} \tag{6}$$

The eigenvalues κ_1 and κ_2 represent the principal curvatures: maximum and minimum. The eigenvectors $\mathbf{k_1}$, $\mathbf{k_2}$ are the corresponding principal directions for the principal curvatures and **n** is the surface normal unit vector at the location of the calculated curvature.

3. Results

Exemplary deformations of the beam at its extreme positions are shown, as 3D renderings, in Figure 5. Changing the amplitude of voltage signal, led to the increase of the maximum deflection. In addition, the shape of the beam became visibly more curved. This was quantified by multiscale curvature analysis. Principal, mean and Gaussian curvatures were calculated at multiple scales. Results of maximum (κ_1) and minimum (κ_2) curvatures calculated for two different scales: nominal, equal to original sampling interval (5 μm) and its twenty-fold multiplier (100 μm) are depicted in Figure 6 for the sample excited at 129.2 μC. Concave features are visible as positive curvature regions, colored with red. Negative curvature (blue) is associated with local convexity. The magnitude of principal, mean and Gaussian curvature decreases with scale. For finer scales, curvature might refer to measurement noise, which might not be charge-dependent phenomenon.

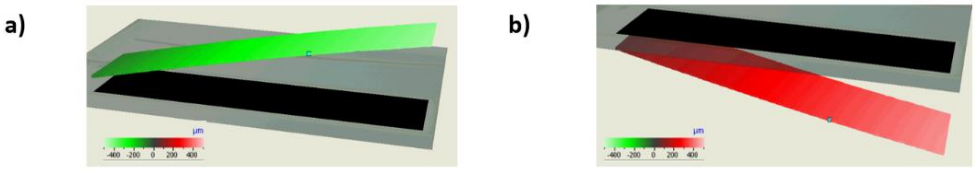

Figure 5. 3D deformations caused by sine signal (U_{in}=13V and f=45Hz – 88.4μC): a) maximal top position and b) maximal bottom position

Statistical measures of principal, mean and Gaussian curvatures for scales between 5 and 125 μm were calculated and correlated together with applied charge using linear regression. Strengths of correlations were plotted versus scale for average and standard deviation of maximum and minimum curvature (fig. 7). Values of coefficient of determination (R^2) did not exceed 0.8 for all parameters except average minimum curvature. Minimum curvature at the largest analyzed scales (>45 μm) can be associated with the general shape of deformed piezoelectric beam and characterizes the bending around the direction aligned with its width. For those large scales, strong correlations with charge are observed.

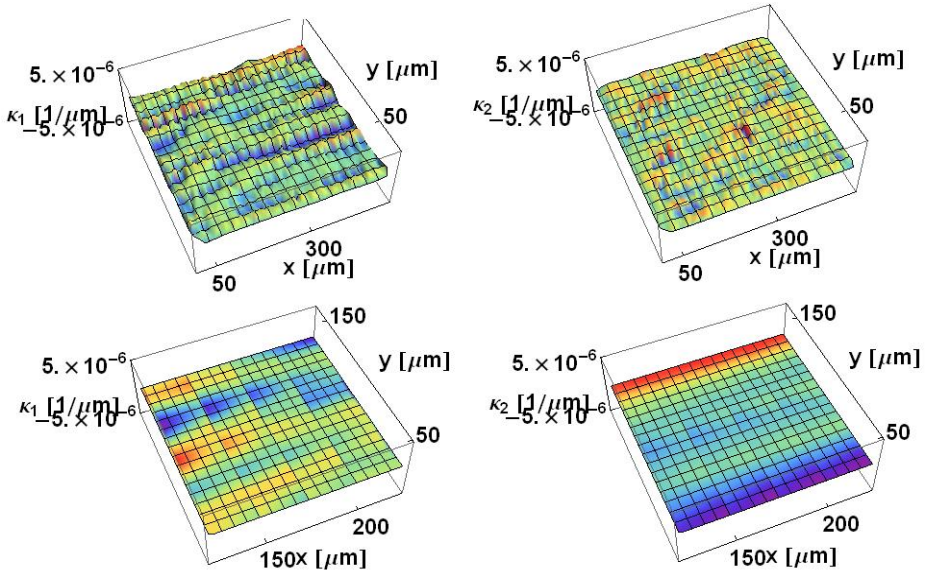

Figure 6. Maximal and minimal curvature calculated at scales 5 μm (upper row) and 100 μm (lower row)

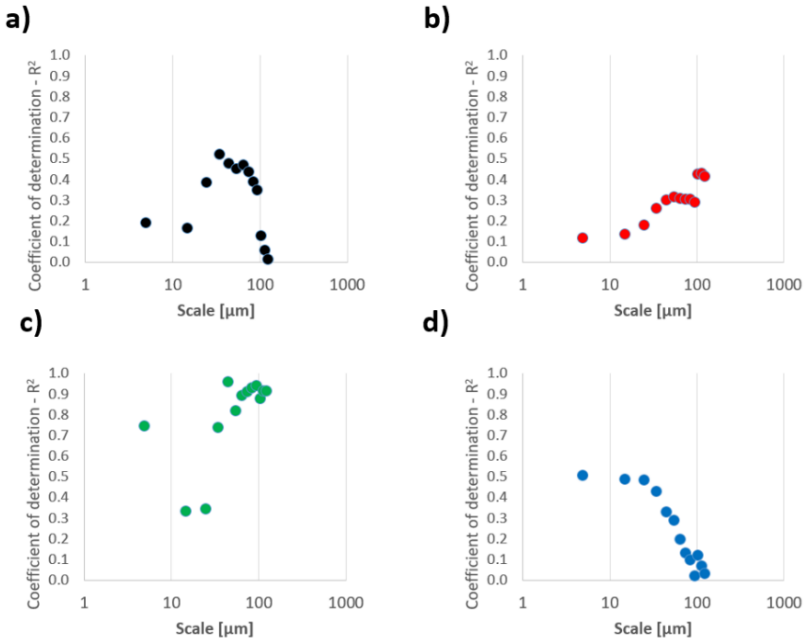

Figure 7. Strengths of correlations between a) mean of κ_1, b) std of κ_1, c) mean of κ_2, d) std of κ_2

Functional relations between average minimum curvature and electric charge are shown, together with coefficient of determination, for four different scales in Figure 8. The data follows an evidently decreasing trend. Negative values of minimum curvature reflect the convex shape what was confirmed visually by inspecting the deformation images (e.g. figure 5 a). The increase of electric charge lead to the growth of negative curvature which might be explained by the larger bending deformations of the beam.

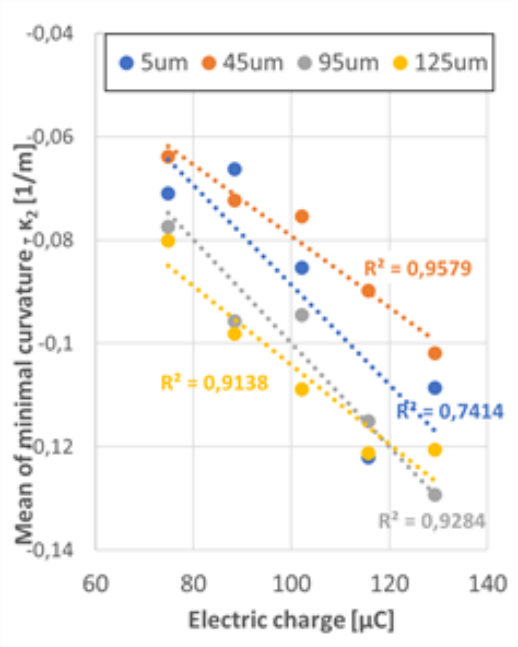

Figure 8. Mean of minimal curvature κ_2 plotted versus charge

4. Conclusion

3D deformations of piezo bimorph actuator under dynamically changed electric charge can be captured using laser 3D vibrometer. The experimental study allowed establishing functional relations between parameter describing the shape of the piezoelement and electric quantity.

Statistical relations between areal curvature and charge were established and strong correlations (R^2>0.8) were found between supplied electric charge to the piezo bimorph actuator and mean of minimum curvature for range of scales between 45 µm and 125 µm. The strongest correlations (R^2=0.96) were observed at scale of 45 µm. Other curvature parameters (maximum, mean and Gaussian) did not correlate well for the analyzed scales.

This study contributes to better understanding of dynamic behavior of piezoelectric components and coupling between electric charge and curvature. Future works will be concentrated on the development of mathematical model of the actuator and its validation by similar experiments.

Acknowledgments

This research was funded by the Polish Ministry of Science and Higher Education as a part of research subsidy – project number: 0614/SBAD/1529.

References

1. R. Cade, *Charge density, vertices and high curvature in two-dimensional electrostatics*, Journal of Electrostatics, 17(2), (1985) 125 – 136.
2. A. R. Hadjesfandiari, *Size-dependent thermoelasticity*, Latin American Journal of Solids and Structures, 11(9) (2016) 1679 – 1708.
3. H. Tamagawa, F. Nogata, M. Sasaki, *Charge quantity as a sole factor quantitatively governing curvature of Selemion*, Sensors and Actuators B, 124 (2007) 6 – 11.
4. V. Kumaran, *Instabilities due to Charge-Density-Curvature Coupling in Charged Membranes*, Physical Review Letters, 85(23) (2000) 4996 – 4999.
5. M. Winterhalter, W. Helfrich, *Effect of surface charge on the curvature elasticity of membranes*, Journal of Physical Chemistry, 92 (1988) 6865 – 6867.
6. V. Vitelli, A. M. Turner, *Anomalous Coupling Between Topological Defects and Curvature*, Physical Review Letters, 93 (21) (2004) 215301-1-4.
7. J. M. Hyde, L. Cadet, J. Montgomery, C. A. Brown, *Multi-scale areal topographic analysis of surfaces created by micro-EDM and functional correlations with discharge energy*, Surf. Topogr.: Metrol. Prop. 2 (2014) 045001.
8. C.A Brown, H. N. Hansen, X. J. Jiang, F. Blateyron, J. Berglund, N. Senin, T. Bartkowiak, B. Dixon, G. Le Goic, Y. Quinsat, W. J. Stemp, *Multiscale analyses and characterizations of surface topographies*, CIRP annals, 67(2) (2018) 839–862.
9. T. Bartkowiak, J. Berglund, C. A. Brown, *Establishing functional correlations between multiscale areal curvatures and coefficients of friction for machined surfaces*, Surface Topography: Metrology and Properties, 6(3) (2018) 034002.
10. T. Bartkowiak, C. A. Brown, A *Characterization of Process–Surface Texture Interactions in Micro-Electrical Discharge Machining Using Multiscale Curvature Tensor Analysis*, ASME. J. Manuf. Sci. Eng., 140(2) (2018) 021013.
11. W. J. Stemp, B. E. Child, S. Vionnet, C.A Brown, *Quantification and discrimination of lithic use-wear: surface profile measurements and length-scale fractal analysis*, Archaeometry, 51 (2009) 366-382.
12. F. Pedreschi, J.M. Aguilera, C.A.Brown, *Characterization of food surfaces using scale-sensitive fractal analysis*,. Journal of Food Process Engineering, 23 (2000) 127-143.
13. R.S. Sayles, T.R. Thomas, *The Spatial Representation of Surface Roughness by Means of the Structure Function: A Practical Alternative to Correlation*, Wear, 42 (1977), 263-276.
14. A.A.G. Bruzzone, J.S. Montanaro, A. Ferrando, P.M. Lonardo, *Wavelet Analysis for Surface Characterisation: an Experimental Assessment*, CIRP Annals—Manufacturing Technology, 53 (1) (2004), 479-482.

15. ISO 25178-2. Geometrical product specifications (GPS)—Surface texture: Areal—Part, 2.
16. J. Berglund, C. Agunwamba, B. Powers, C.A. Brown, B.-G. Rosén, *On Discovering Relevant Scales in Surface Roughness Measurement—An Evaluation of a Band-Pass Method*, Scanning, **32** (2010), 244-249.
17. D. Gogolewski, *Influence of the edge effect on the wavelet analysis process, Measurement*, **152** (2020), 107314.
18. B.B. Mandelbrot, *The Fractal Geometry of Nature*, W.H Freeman and Co., San Francisco, CA (1982).
19. X. Zhang, Y. Xu, R.L. Jackson, *An Analysis of Generated Fractal and Measured Rough Surfaces in Regards to Their Multiscale Structure and FD*, Tribology International, **105** (2017), 94-101.
20. A. Milecki, M. Pelic, *Application of geometry based hysteresis modelling in compensation of hysteresis of piezo bender actuator*, Mechanical Systems and Signal Processing, **78** (2016) 4 – 17.
21. A. Pressley, *Elementary Differential Geometry*, Springer-Verlag London 2010.
22. T. Bartkowiak, C. A. Brown, *Multiscale 3D Curvature Analysis of Processed Surface Textures of Aluminum Alloy 6061 T6*. Materials , **12(2)** (2019) 257.